Desalination and Water Treatment
www.deswater.com

doi: 10.5004/dwt.2022.28969

277 (2022) 85–89
November

Adsorption of Covid-19-related drug from contaminated water using activated carbon

Luís Fernando Cusioli*, Daniel Mantovani, Heloise Beatriz Quesada,
Raquel Guttierres Gomes, Rosângela Bergamasco

Department of Chemical Engineering, State University of Maringa, Maringa 87020-900, Parana, Brazil, Tel. +554430114782; emails: luiscusioli@gmail.com.br. (L.F. Cusioli), daniel26mantovani@gmail.com.br (D. Mantovani), heloisequesada@gmail.com.br (H.B. Quesada), rgutti02@gmail.com (R. Guttierres Gomes), rosangela@deq.uem.br (R. Bergamasco)

Received 31 July 2022; Accepted 4 October 2022

ABSTRACT

Chloroquine has been adopted in some countries such as Brazil as a Covid-19 prevention protocol; consequently, chloroquine has contaminated water resources in large quantities. In response to this menace, an adsorbent material from animal bone was used to remove chloroquine from contaminated water. Notably, no drug adsorption studies have been conducted in the past. The adsorbent was characterized by scanning electron microscopy and zeta potential measurements that exhibited favorable characteristics for the adsorbent. In this study, it was determined that the optimal mass of the adsorbent was 0.02 g at pH 7. The kinetic study demonstrated that 300 min was sufficient to reach equilibrium, and the best fit was pseudo-second-order. The adsorption isotherms were fitted in the Langmuir model, obtaining a maximum adsorption capacity of 77.60 mg^{-1} at a temperature of 298 K. The thermodynamic parameters demonstrated a spontaneous, exothermic, and reversible process. Briefly, the adsorbent used had the potential to remove emerging pollutants from the environment.

Keywords: Activated carbon; Covid-19; Chloroquine; Emerging pollutants

1. Introduction

The outbreak of the Covid-19 pandemic led to the onset of serious problems caused by the virus and the rampant use of inefficient medications such as chloroquine for the prevention of the virus [1]. Some countries have adopted chloroquine as a Covid-19 prevention protocol, and with its high consumption [2], a large environmental impact has been caused mainly by the contamination of water bodies, as the drugs are not fully metabolized and end up being excreted and released to the environment [3]. To remove these compounds from the environment, some types of treatments are efficient, and the adsorption process stands out [4].

The traces of drugs that reach water bodies can be efficiently removed through adsorption, and some of the advantages of using this process is that it is simple, easy-to-operate, and low-cost [5]. Choosing a good adsorbent should be based on its characteristics. For good adsorption results, it must contain high carbon content, abrasion resistance, thermal stability and small diameter pores, which results in an elevation of the contact surface, and therefore, adsorption capacity. Therefore, it is important to carry out a structural characterization of the adsorbent to assess its pollutant retention capacity [6,7]. Given the problem presented by the subject, this study sought to evaluate the removal of chloroquine using commercial activated charcoal from an animal source.

---

* Corresponding author.

2. Materials and methods

Activated charcoal from animal bone was donated by Carbontec® headquartered in the city of Maringá, Brazil. The material was morphologically characterized through scanning electron microscopy (SEM) (Quanta 250 FEI), and the surface zeta potential of the newly developed material was analyzed using a particle analyzer, DelsaNanoC (Beckman Coulter).

All adsorption experiments were performed in duplicate with the aid of a shaking table (Tecnal) at 150 rpm. Five conditions (0.01, 0.02, 0.03, 0.04, and 0.05 g) were used to evaluate the mass effect. For the effect of pH, values of 4, 7, and 10 were employed. For both investigations, chloroquine solutions (CLQ) at 20 mg·L^{-1} [8] were used, with a total contact time of 24 h at 25°C. The study kinetics were performed with CLQ concentration of mg·L^{-1}, removing aliquots within a time interval ranging from 1 to 500 min. In the adsorption isotherms, the variations in the concentrations of CLQ (5–90 mg·g^{-1}) at temperatures of 298, 308, and 318 K were evaluated. After the stipulated contact time for each experiment, filtration was performed using a 0.45 μm cellulose acetate membrane (Unifil). All CLQ concentrations were measured using a spectrophotometer (HACH DR 5000) at 280 nm.

3. Results and discussion

SEM demonstrated the morphological structure and consequently the porosity of the material studied at a magnification of 2,000x as shown in Fig. 1.

As shown in Fig. 1, the pore cavities are heterogeneous and may have numerous active sites, facilitating the adsorption of the contaminant to the material [9]. The zeta potential was determined to obtain a deeper understanding of the surface charge of the material, as shown in Fig. 2.

It was observed that the adsorbent exhibited several negative charges in the studied pH range. The positive charges are separated from the negative charges at the line of origin and the point that crosses this origin is known as the isoelectric point, occurring at approximately pH 3. At pH > 3, the adsorbent exhibited negative charges, and at pH < 3, it exhibited positive charges [10]. The experiments for determining the optimal mass and pH are presented in Fig. 3A and B.

To study the effect of mass, the amount of adsorbent in 0.01, 0.02, 0.03, 0.04, and 0.05 g was varied. As shown in Fig. 3A, the following adsorption capacities were obtained: 50.52, 28.40, 19.94, 14.50, and 11.47 mg·g^{-1}, and removal percentages of 84.20%, 94.65%, 99.70%, 96.65%, and 95.60%, respectively. Therefore, a mass of 0.02 g was selected to be

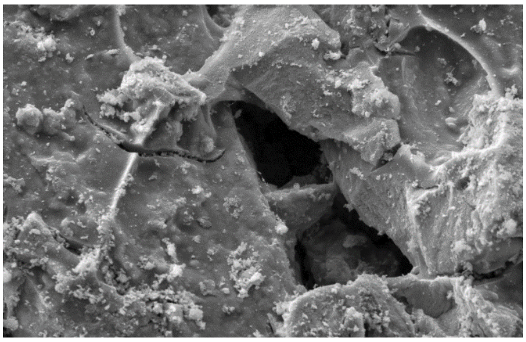

Fig. 1. SEM of active charcoal from animal bone.

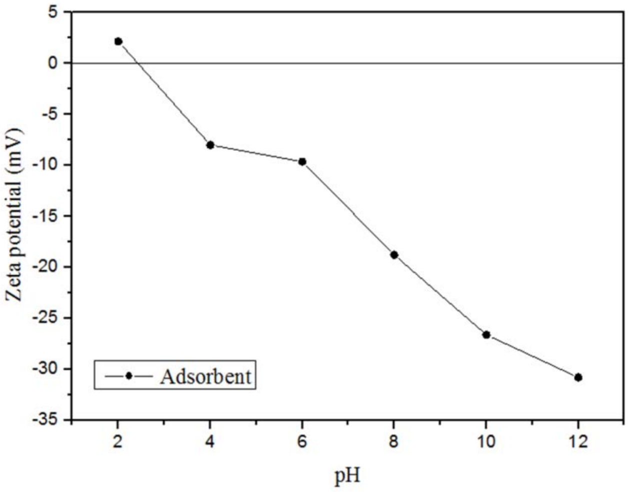

Fig. 2. Zeta potential of the adsorbent.

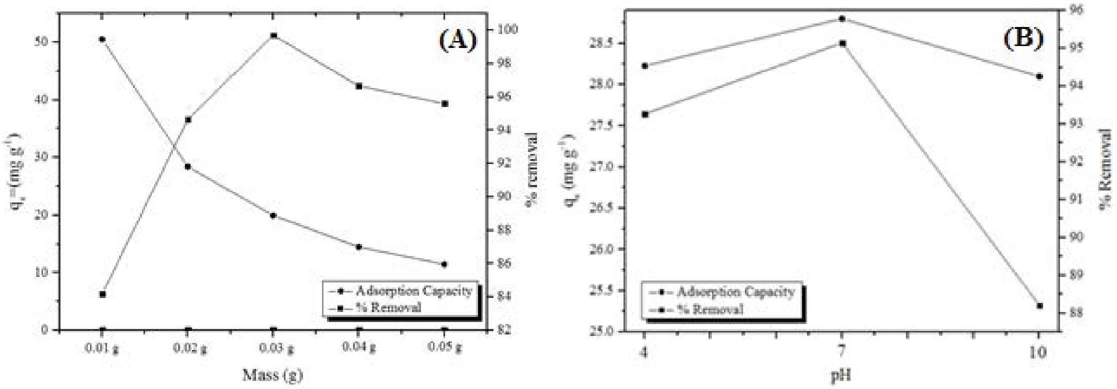

Fig. 3. (A) Adsorbent variation from animal bone and (B) chloroquine solution pH variation.

used in the other tests [11]. The effect of the pH of the CLQ was studied at 4, 7, and 10 pH levels, obtaining adsorption capacities of 28.23, 28.80, and 26.70 mg·g^{-1}, and removal percentages of 93.26%, 95.14%, and 88.21%, respectively. Thus, the optimal pH of the experiment was determined as 7 [12].

Fig. 4 demonstrates the kinetic relationship between the adsorbent and the adsorbate, and it was verified that the equilibrium occurred at approximately 300 min with an adsorption capacity of 28,855 mg·g^{-1} and a removal percentage of 95.67%. The two classical mathematical models were applied to the experimental data: pseudo-first-order and pseudo-second-order, whose parameters are listed in Table S1. The values of the correlation coefficient (R^2) were 0.968 for pseudo-first-order and 0.984 for pseudo-second-order. The calculated adsorption capacities were 33,366 mg·g^{-1} for pseudo-first-order and 28,788 mg·g^{-1} for pseudo-second-order, indicating that the value obtained by the last model was almost equal to the experimental value (q_e). Furthermore, the chi-square value (χ^2) was lower (0.012) than that of pseudo-first-order (0.132). This fact demonstrates the determination of the pseudo-second-order model to represent the data obtained experimentally, suggesting that the adsorption process is limited by chemisorption [13–15].

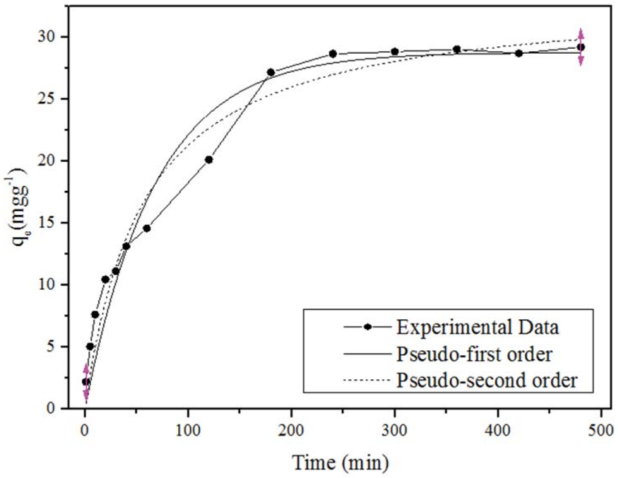

Fig. 4. Adsorption kinetics of CLQ with the adsorbent.

The adsorption isotherms are shown in Fig. 5 in which the Langmuir and Freundlich models were applied. The values obtained are listed in Table S2. The R^2 values for the Langmuir model were 0.990, 0.977, and 0.963 for 298, 308, and 318 K, respectively, which are higher than the R^2 obtained by the Freundlich model. In the Langmuir model, the maximum adsorption capacities (q_{max}) were 77.60, 69.88, and 52.06 mg·g^{-1}, respectively. Therefore, this model was the best fit, and it assumes that the adsorption process occurred in a monolayer and there is a defined number of active sites that help in the retention of an adsorbate molecule and prevents it from interacting with other molecules [16].

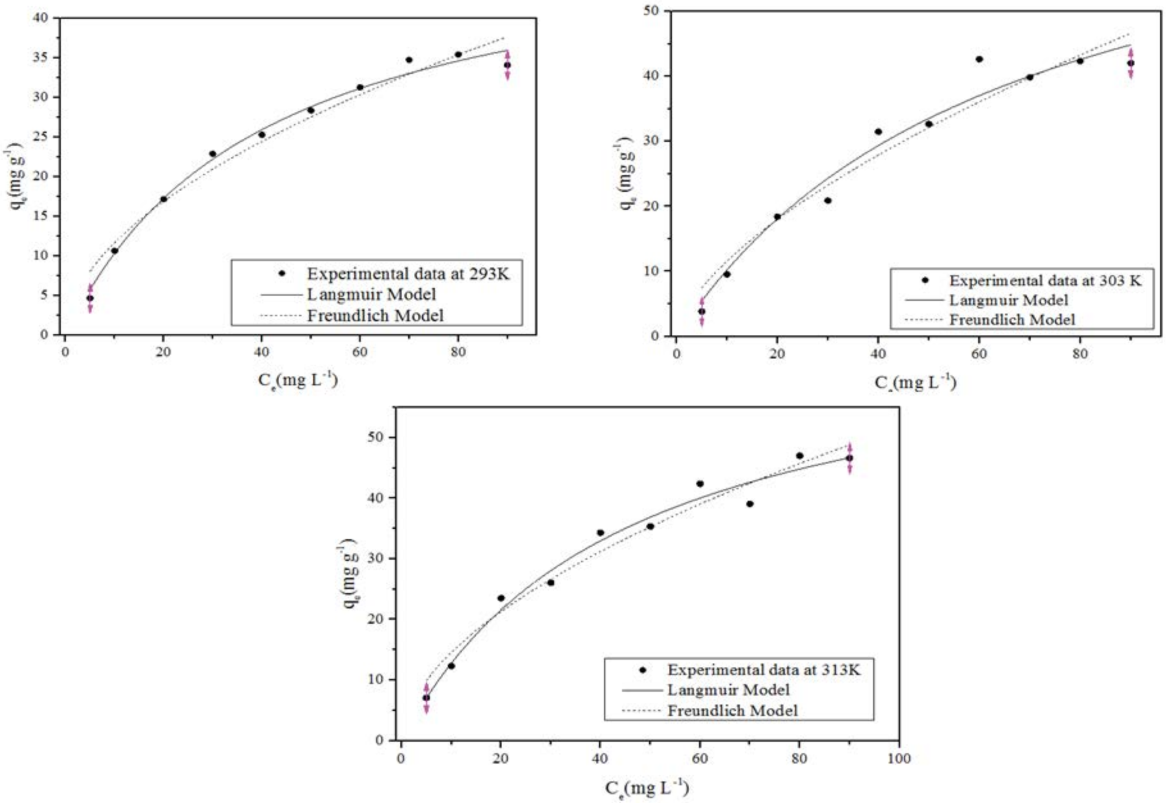

Fig. 5. CLQ adsorption isotherms on the adsorbent.

The thermodynamic parameters were calculated using the results obtained in the equilibrium study. K_C values were determined using the Langmuir constant [17]. The variances in Gibbs free energy (ΔG), enthalpy (ΔH), and entropy (ΔS) are summarized in Table S3. It was observed that the studied temperatures had a variation in the negative Gibbs free energy, demonstrating that the adsorption process occurred spontaneously and favorably. The negative value of ΔH suggested that the process was exothermic, unfavorable with increasing temperature, and the value of –5.01 kJ·mol^{-1} indicated that the adsorption process occurred through physiosorption mechanisms. The low and positive value of ΔS (0.06 kJ·mol^{-1}) demonstrated that the interaction between CLQ and animal bone adsorbent occurred randomly through the solid–liquid interface.

4. Conclusion

Animal bone char was analyzed using SEM images in which it was verified that it has heterogeneous porosity, a characteristic that facilitates the adsorption of CLQ. The zeta potential indicated that the isoelectric point was at pH 3. The mass effect established that the mass of 0.02 g of adsorbent obtained a q_e of 28.40 mg·g^{-1} and the best pH for the study was 7. The kinetic study confirmed that stability occurred at approximately 300 min, and the best fitted model was the pseudo-second-order. The adsorption isotherms were fitted in the best Langmuir model with a $q_{\max}$ of 77.60 mg·g^{-1} at a temperature of 298 K. Thermodynamic parameters indicated that the process was exothermic, spontaneous, and had an excellent solid–liquid interface. The adsorption studies revealed that the adsorbent in question was efficient for the chloroquine adsorption process, and the importance of this material is highlighted because no adsorption studies of the drug have been conducted thus far.

Acknowledgments

The authors thank the National Council for Scientific and Technological Development (CNPq), the Higher Education Personnel Improvement Coordination (CAPES), and Carbontec® for providing the material for the study.

Conflict of interest

The authors declare that they have no conflict of interest.

Data availability

Not applicable.

References

[1] H. Jahrami, A.S. BaHammam, N.L. Bragazzi, Z. Saif, M. Faris, M.V. Vitiello, Sleep problems during the COVID-19 pandemic by population: a systematic review and meta-analysis, J. Clin. Sleep Med., 17 (2021) 299–313.

[2] F. Sevilla-Castillo, O.J. Roque-Reyes, F. Romero-Lechuga, M.F. Gómez-Núñez, M. Castillo-López, D. Medina-Santos, P.O. Román, J.R. Flores-Hernández, J.D. Méndez-Coca, D. Montaño-Olmos, K.C. Farfán-Lazos, M. Tobón-Cubillos, A. Viveros-Hernández, L. Torres-Ortega, K.Y. Hernández-Skewes, G. Montiel-Bravo, S. Ortega-Rodríguez, A.N. Peón, Both chloroquine and lopinavir/ritonavir are ineffective for COVID-19 Treatment and combined worsen the pathology: a single-center experience with severely ill patients, BioMed Res. Int., 2021 (2021) 8821318, doi: 10.1155/2021/8821318.

[3] C.D. Metcalfe, A.C. Alder, B. Halling-Sørensen, K. Krogh, K. Fenner, M. Larsbo, J.O. Straub, T.A. Ternes, E. Topp, D.R. Lapen, A.B.A. Boxall, Exposure Assessment Methods for Veterinary and Human-Use Medicines in the Environment: PEC vs. MEC Comparisons, K. Kümmerer, Eds., Pharmaceuticals in the Environment, Springer, Berlin, Heidelberg, 2008, pp. 147–171, doi: 10.1007/978-3-540-74664-5_11.

[4] J. Qu, Research progress of novel adsorption processes in water purification: a review, J. Environ. Sci., 20 (2008) 1–13.

[5] M. Grassi, G. Kaykioglu, V. Belgiorno, G. Lofrano, Removal of Emerging Contaminants from Water and Wastewater by Adsorption Process, G. Lofrano, Ed., Emerging Compounds Removal from Wastewater, SpringerBriefs in Molecular Science, Springer, 2012, pp. 15–37, doi: 10.1007/978-94-007-3916-1_2.

[6] I. Ali, M. Asim, T.A. Khan, Low cost adsorbents for the removal of organic pollutants from wastewater, J. Environ. Manage., 113 (2012) 170–183.

[7] Y. Liu, X. Zhang, J. Wang, A critical review of various adsorbents for selective removal of nitrate from water: structure, performance and mechanism, Chemosphere, 291 (2022) 132728, doi: 10.1016/j.chemosphere.2021.132728.

[8] J. Liu, R. Cao, M. Xu, X. Wang, H. Zhang, H. Hu, Y. Li, Z. Hu, W. Zhong, M. Wang, Hydroxychloroquine, a less toxic derivative of chloroquine, is effective in inhibiting SARS-CoV-2 infection in vitro, Cell Discovery, 6 (2020), doi: 10.1038/s41421-020-0156-0.

[9] K.S.W. Sing, Adsorption methods for the characterization of porous materials, Adv. Colloid Interface Sci., 76–77 (1998) 3–11.

[10] J.D. Clogston, A.K. Patri, Zeta Potential Measurements, Methods Mol. Biol., 2011, doi: 10.1007/978-1-60327-198-1_6.

[11] S. Eris, S. Azizian, Extension of classical adsorption rate equations using mass of adsorbent: a graphical analysis, Sep. Purif. Technol., 179 (2017) 304–308.

[12] A. Farooq, L. Reinert, J.M. Levêque, N. Papaiconomou, N. Irfan, L. Duclaux, Adsorption of ionic liquids onto activated carbons: effect of pH and temperature, Microporous Mesoporous Mater., 158 (2012) 55–63.

[13] W. Plazinski, J. Dziuba, W. Rudzinski, Modeling of sorption kinetics: the pseudo-second-order equation and the sorbate intraparticle diffusivity, Adsorption, 19 (2013) 1055–1064.

[14] J. Wang, X. Guo, Adsorption kinetic models: physical meanings, applications, and solving methods, J. Hazard. Mater., 390 (2020) 122156, doi: 10.1016/j.jhazmat.2020.122156.

[15] X. Guo, J. Wang, A general kinetic model for adsorption: theoretical analysis and modeling, J. Mol. Liq., 288 (2019) 111100, doi: 10.1016/j.molliq.2019.111100.

[16] J. Wang, X. Guo, Adsorption isotherm models: classification, physical meaning, application and solving method, Chemosphere, 258 (2020) 127279, doi: 10.1016/j.chemosphere.2020.127279.

[17] É.C. Lima, M.A. Adebayo, F.M. Machado, Kinetic and Equilibrium Models of Adsorption, C. Bergmann, F. Machado, Eds., Carbon Nanomaterials as Adsorbents for Environmental and Biological Applications, Carbon Nanostructures, Springer, Cham, 2015, pp. 33–69, doi: 10.1007/978-3-319-18875-1.

Supplementary information

The adsorption capacity (q_e) was calculated from Eq. (S1):

$$q_t = \frac{C_0 - C_t}{m} V \tag{S1}$$

where q_t is the amount of chloroquine (CLQ) adsorbed at time t (mg·g^{-1}), V is the volume of the solution (L) and m is the mass of the adsorbent (g).

The kinetic data was fitted into pseudo-first-order and pseudo-second-order models, represented in Eqs. (2) and (3), respectively [S1,S2].

$$q_t = -\exp\left(-K_1 \cdot t\right) \cdot q_e + q_e \tag{S2}$$

$$q_t = \frac{k_2 \cdot q_e^2}{1 + k_2 \cdot q_e \cdot t} \tag{S3}$$

Table S1
Kinetic parameters of CLQ adsorption onto adsorption

Kinetic models	Estimated parameters values	Experimental data
Pseudo-first-order	q_{eq} (mg·g^{-1})	33.366
	k_1 (min^{-1})	0.015
	R^2	0.968
	χ^2	0.132
Pseudo-second-order	q_{eq} (mg·g^{-1})	28.788
	k_2 (g·mg^{-1}·min^{-1})	0.004
	R^2	0.984
	χ^2	0.012

Table S2
Equilibrium parameters of CLQ adsorption onto adsorption

Isotherm model	Parameters	298 K	308 K	318 K
Langmuir	$q_{\max}$ (mg·g^{-1})	77.60	69.88	52.06
	K_L (L·mg^{-1})	0.025	0.022	0.015
	R^2	0.990	0.977	0.963
Freundlich	K_F (mg·g^{-1})(mg·L^{-1})^{nF}	1.18	1.58	1.81
	n_F	3.423	2.703	4.085
	R^2	0.962	0.938	0.962

Table S3
Thermodynamic parameters of CLQ adsorption onto adsorption

T (°C)	T (K)	$\Delta G°$ (kJ·mol^{-1})	$\Delta H°$ (kJ·mol^{-1})	$\Delta S°$ (kJ·mol^{-1})
25	298	–22.02	–5.01	0.06
35	308	–22.65		
45	328	–23.16		

where q_t and q_e are the adsorption capacities at time t and equilibrium (mg·g^{-1}), t is the time (min), k_1 (min^{-1}) is the constant of the adsorption rate of pseudo-first-order and k_2 (g·mg^{-1}·min^{-1}) is the pseudo-second-order adsorption rate constant.

The equilibrium data were fitted into the Langmuir and Freundlich isotherm models [S3,S4], presented in Eqs. (S4) and (S5), respectively.

$$q_e = \frac{q_m \cdot k_L \cdot C_e}{\left(1 + k_L \cdot C_e\right)} \tag{S4}$$

$$q_e = K_F \cdot C_e^{1/n} \tag{S5}$$

where q_e (mg·g^{-1}) is the adsorption capacity at equilibrium, C_e is the concentration at equilibrium (mg·L^{-1}), K_L (mg·g^{-1}) is the Langmuir equilibrium constant and n and K_F ((mg·g^{-1}) (L·mg^{-1})$^{1/n}$) are Freundlich constants that represent the intensity and the adsorption capacity, respectively.

Concerning the thermodynamic parameters, Gibbs free energy is directly calculated from Eq. (S6).

$$\Delta G° = -RT \ln K_C \tag{S6}$$

where $\Delta G°$ is the Gibbs free energy (kJ·mol^{-1}), R is the ideal gas constant (8.314 J·mol^{-1}·K^{-1}), T is the temperature (K) and K_C is the equilibrium constant.

The enthalpy and entropy are calculated from Eq. (S7). These parameters are obtained from the angular and linear coefficient of the graph lnK_C vs. $1/T$. It is possible to calculate K_C it from the Langmuir constant, considered the most coherent in recent works [S5,S6].

$$\ln K_C = \frac{\Delta S}{R} - \frac{\Delta H}{RT} \tag{S7}$$

where $\Delta G°$ and $\Delta H°$ are the Gibbs free energy and enthalpy (kJ·mol^{-1}); $\Delta S°$ is the entropy (kJ·mol^{-1}·K^{-1}); T is the temperature (K) and K_C is the equilibrium constant.

References

[S1] Y.S. Ho, G. McKay, Pseudo-second-order model for sorption processes, Process Biochem., 34 (1999) 451–465.

[S2] Y.S. Ho, G. McKay, A comparison of chemisorption kinetic models applied to pollutant removal on various sorbents, Process Saf. Environ. Prot., 76 (1998) 332–340.

[S3] I. Langmuir, The constitution and fundamental properties of solids and liquids, J. Am. Chem. Soc., 38 (1917) 2221–2295.

[S4] H.M. Freundlich, Over the adsorption in solution, J. Phys. Chem., 57 (1906) 385–470.

[S5] É.C. Lima, M.A. Adebayo, F.M. Machado, Kinetic and Equilibrium Models of Adsorption, C. Bergmann, F. Machado, Eds., Carbon Nanomaterials as Adsorbents for Environmental and Biological Applications, Carbon Nanostructures, Springer, Cham, 2015, pp. 33–69, doi: 10.1007/978-3-319-18875-1.

[S6] H.N. Tran, S.J. You, A. Hosseini-Bandegharaei, H.P. Chao, Mistakes and inconsistencies regarding adsorption of contaminants from aqueous solutions: a critical review, Water Res., 120 (2017) 88–116.